J Solid State Electrochem (2003) 7: 201–207
DOI 10.1007/s10008-002-0301-8

ORIGINAL PAPER

Seung-Bok Lee · Su-Il Pyun

Critical assessment of a new in situ spectroelectrochemical cell designed for the study of interfacial reactions between a porous graphite anode and alkyl carbonate solution

Received: 21 March 2002 / Accepted: 11 June 2002 / Published online: 2 August 2002

Abstract This article critically evaluates the characteristics of a new in situ spectroelectrochemical cell with an optimized path of the IR beam, designed in our laboratory for study of the solid electrolyte interphase (SEI) layer formed between a porous graphite anode and alkyl carbonate solution for lithium-ion batteries. The cell was designed in view of the optical principles underlying the way the in situ cell works, to give depth of penetration of the evanescent IR beam through the attenuated total internal reflectance crystal into the electrolyte at such a small value, ranging from 0.277 to 2.77 μm, that it was possible to minimize the "masking effect" of the ethylene carbonate/diethyl carbonate solvent. Moreover, the "local compositional change" which may arise significantly from the "thin layer electrolyte configuration" cell also could be fairly avoided, since only the electrolyte in the vicinity of the electrode composed of graphite particles is reduced to form the SEI layer to a thickness of at most 0.1 μm during the application of potentials. Thus, it was possible to measure the in situ FT-IR spectra in the cell, which represents the real chemical composition and structure of the SEI layer. Taking the application of the designed in situ cell as an example, this article reports the effect of salt type and electrolyte temperature on the chemical composition and structure of the SEI layer between graphite particles and alkyl carbonate solution with the help of various measured in situ FT-IR spectra.

Keywords Fourier transform infrared · Spectroelectrochemistry · Attenuated total internal reflectance · Solid electrolyte interphase · Graphite anode

S.-B. Lee · S.-I. Pyun (✉)
Department of Materials Science and Engineering,
Korea Advanced Institute of Science and Technology,
373-1 Guseong-dong, Yuseong-gu 305-701,
Daejeon, Republic of Korea
E-mail: sipyun@mail.kaist.ac.kr
Tel.: +82-42-8693319
Fax: +82-42-8693310

Introduction

In situ Fourier transform infrared (FT-IR) spectroelectrochemistry has proven useful for elucidating the structure of chemical intermediates and studying the redox chemistry of a wide range of molecules. In the past, many spectroelectrochemical cells for in situ FT-IR spectroscopy have been proposed and developed [1, 2, 3, 4, 5, 6]. These designs range from transmission electrochemical cells to designs utilizing reflectance methods. With transmission electrochemical cells, using minigrid electrodes, one measures the FT-IR spectra of the electrochemical species in the bulk solution [7, 8]. In contrast, with most reflectance methods, one measures the FT-IR spectra of the electrochemical species near or on the electrode surface, with either a totally reflective electrode [9, 10] or a transparent electrode [11].

When measuring IR reflectance spectra from a liquid/solid interface, using the attenuated total internal reflectance (ATR) method or the single internal reflectance (SIR) method, the main difficulty is the "masking effect" of most solvents, which means the absorption of the IR radiation significantly arises by itself [12]. To circumvent this problem, "thin layer electrolyte configuration" cells, which are characteristic of the arrangement for a very thin layer of electrolytic solution between the electrode and the IR window, were first proposed by Bewick et al. [13, 14]. However, when the electrochemical reaction between the electrode and the "electrolyte with a thin layer" runs very fast in the "thin electrolyte layer configuration" cell, the composition of the reactant within the thin layer of the electrolyte may be depleted as compared to the composition in the bulk electrolyte. For the sake of avoiding the "local compositional change" between the thin layer electrolyte and the bulk electrolyte, many types of in situ spectroelectrochemical cell have been developed [15, 16, 17].

In particular, the use of in situ FT-IR spectroelectrochemistry made it possible to clearly specify the chemical composition and structure of the solid electrolyte

interphase (SEI) layer formed between a porous graphite anode and alkyl carbonate solution for lithium-ion secondary batteries. Measurement of the ex situ FT-IR spectra leads to the interference of secondary reactions of the SEI layer with such atmospheric contaminants as H_2O or CO_2, unavoidably present in the spectrometer environment. In addition, several salt reduction products may have quite similar FT-IR peaks to the parent salts. Therefore, the appearance of certain noise peaks in the FT-IR spectra measured ex situ may always be attributed to the residual salt that is not completely washed out during the specimen preparation for ex situ FT-IR spectroscopy. The occurrence of the noise peak is effectively avoided when the electrodes are subjected to in situ FT-IR spectroscopic measurement [18, 19, 20].

The purpose of this article is to introduce a new in situ FT-IR spectroelectrochemical cell with an optimized path of the IR beam, designed in our laboratory for the study of the chemical composition and structure of the SEI layer between a porous graphite electrode and the alkyl carbonate solution. For this purpose, we first detailed how we minimized the "masking effect" of the solvent as well as how we circumvented the "local compositional change" in the new in situ cell. Finally, we measured in situ FT-IR spectra with the newly designed in situ cell and analysed them in order to illustrate the effect of salt type and electrolyte temperature on the chemical composition and structure of the SEI layer as examples.

Experimental

Design of a new spectroelectrochemical cell for in situ FT-IR spectroscopy

The new in situ spectroelectrochemical cell with an optimized path of the IR beam is schematically illustrated in Fig. 1. The in situ cell was constructed by attaching the baseline horizontal ATR crystal attachment to the electrochemical cell. Two kinds of porous graphite electrodes prepared from poly(vinylidene fluoride) (PVDF)-bonded Lonza KS-44 and SLX6 graphite powders were in mechanical contact with the ATR crystal, and they were used as working electrodes. The porous graphite electrode, of which the thickness was measured to be ca. 100 μm, was completely wetted by the penetrated electrolyte. Pure lithium metal foil was employed as the reference and counter electrodes. The two kinds of electrolytes were 1 M $LiPF_6$ in ethylene carbonate (EC)/diethyl carbonate (DEC) (50:50 vol%) solution and 1 M $LiAsF_6$ in EC/DEC solution. The cell configuration and electrode preparation method were detailed in our previous paper [20].

Figure 1a gives a magnified view showing the trace of the IR beam within the 60° cut ATR crystal during its total internal reflections. The IR beam passes from the IR source via a reflecting mirror through the ATR crystal to the deuterated triglycine sulfate (DTGS) detector. In order for the IR beam to totally internally reflect within the ATR crystal, the angle of the incident radiation θ must exceed the critical angle, θ_c. θ_c is a function of the refractive indices of the specimen and the ATR crystal and is defined as [21]:

$$\theta_c = \sin^{-1}\frac{n_2}{n_1} \tag{1}$$

where n_1 is the refractive index of the ATR crystal and n_2 is the refractive index of the specimen. In the case of the newly designed in situ cell, the refractive indices of the ATR crystal (ZnSe prism) and most alkyl carbonate solutions are given by 2.4 and ca. 1.5, respectively. Therefore, θ_c was determined to be 38.7° from Eq. 1.

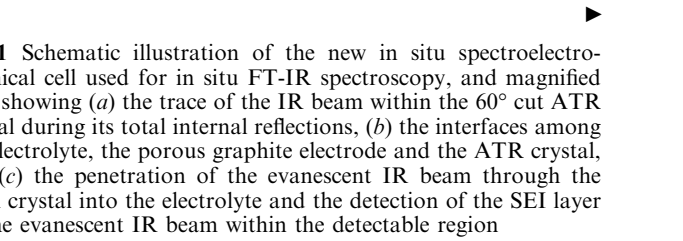

Fig. 1 Schematic illustration of the new in situ spectroelectrochemical cell used for in situ FT-IR spectroscopy, and magnified view showing (*a*) the trace of the IR beam within the 60° cut ATR crystal during its total internal reflections, (*b*) the interfaces among the electrolyte, the porous graphite electrode and the ATR crystal, and (*c*) the penetration of the evanescent IR beam through the ATR crystal into the electrolyte and the detection of the SEI layer by the evanescent IR beam within the detectable region

Another useful relationship in ATR spectroscopy, which can be used as a measure of the depth of the penetration of the evanescent wave through the ATR crystal into the specimen, is defined as the penetration depth d_p. The penetration depth is defined as the distance from the ATR crystal/specimen interface to a location where the intensity of the evanescent wave decays to 1/e of its original value. It is derived by [22]:

$$d_p = \frac{\lambda}{2\pi n_1\sqrt{\sin^2\theta - \left(\frac{n_2}{n_1}\right)^2}} \tag{2}$$

where λ is the wavelength of the IR beam, and θ is the angle of incidence.

From Eq. 2 it is realized that the penetration depth of the IR beam is decreased, and hence the "masking effect" of the solvent is reduced with an increasing incident angle of the IR beam during total internal reflection, which enables us to measure more accurately the chemical composition and structure of even a very thin SEI layer of 0.1 μm thickness. In contrast, the number of total internal reflections within the crystal is decreased with increasing incident angle of the IR beam, which makes the resolution of the measured IR spectra much lower and simultaneously improves the sensitivity of the measured IR spectra. Compromising the decrease in the penetration depth with the decrease in the number of total internal reflections, from the two viewpoints mentioned above, the incident angle was calculated to be 60°. Therefore, we employed the 60° cut ATR crystal as the optimum cut geometry for the study of the very thin SEI layer formed between the porous graphite electrode and the alkyl carbonate solution.

Since the incident angle of 60° of the IR beam is higher than the critical angle for total internal reflectance (38.7°), the incident IR beam is first totally internally reflected within the 60° cut ATR crystal on one beveled plane of the ATR crystal, followed by seven times of total internal reflections on the basal plane of the ATR crystal, and finally the beam is totally internally reflected on the other beveled plane. This internal reflection creates an evanescent wave which extends beyond the surface of the ATR crystal into the specimen. In the regions of the IR spectrum where the surface species absorbs energy, the evanescent wave is attenuated.

Figure 1b schematically presents a magnified view representing the interfaces among the electrolyte, the porous graphite electrode and the ATR crystal. At the same time, Fig. 1c schematically illustrates the penetration of the evanescent IR beam through the ATR crystal into the electrolyte and the detection of the SEI layer by the evanescent IR beam within the detectable region. Considering the cut geometry of the ATR crystal and the reflective indices of the ATR crystal and electrolyte, the penetration depth of the IR beam was determined to 0.277–2.77 μm from Eq. 2, taking the value of the wavelength as 2.5–25 μm, respectively. This means that the penetration depth is much shallower as compared with the thickness of the porous graphite electrode of ca. 100 μm, and at the same time it is comparable with the thickness of the SEI layer of ca. 0.1 μm. Owing to the short penetration depth of the IR beam, the designed in situ cell can be regarded as one variant of the "thin layer electrolyte configuration" cells, and hence the "masking effect" of the solvent can be minimized.

At the same time, it should be noted that only the reactant contained in the electrolyte penetrated into the porous graphite electrode, which is directly in contact with graphite particles and is

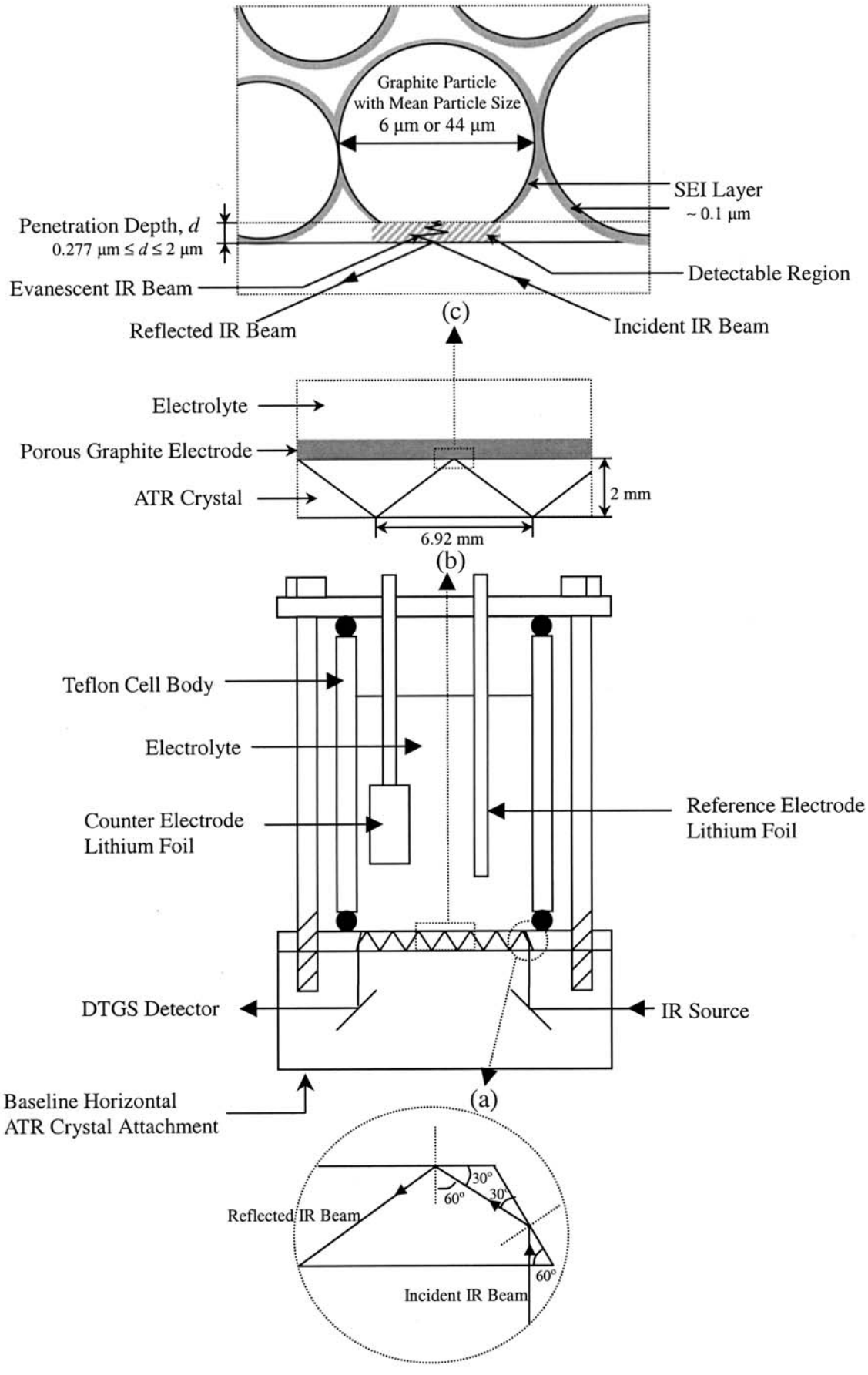
Graphite Particle
with Mean Particle Size
6 μm or 44 μm
SEI Layer
~ 0.1 μm
Penetration Depth, d
0.277 μm ≤ d ≤ 2 μm
Evanescent IR Beam
Detectable Region
Reflected IR Beam
Incident IR Beam
(c)
Electrolyte
Porous Graphite Electrode
ATR Crystal
2 mm
6.92 mm
(b)
Teflon Cell Body
Electrolyte
Counter Electrode
Lithium Foil
Reference Electrode
Lithium Foil
DTGS Detector
IR Source
Baseline Horizontal
ATR Crystal Attachment
(a)
30°
60°
30°
Reflected IR Beam
60°
Incident IR Beam

reduced to develop a reduction product layer, i.e. the SEI layer. This layer extends to ca. 0.1 μm in thickness (see Fig. 1c). Since the SEI layer is widely distributed over the porous graphite electrode, the composition of the reactant contained in the penetrated electrolyte and the bulk electrolyte is scarcely locally changed as a whole. Thus the "local compositional change" which may arise significantly from the "thin layer electrolyte configuration" cell could be fairly avoided in the newly designed in situ cell with an optimized path of the IR beam.

In this respect, in the case of the use of the porous graphite electrode as a working electrode, we can effectively minimize the "masking effect" of the solvent as well as avoid the "local compositional change" by controlling the penetration depth of the IR beam. Thus, it was possible to measure the in situ FT-IR spectra which represent the real chemical composition and structure of the SEI layer within the detectable region using the spectroelectrochemical cell.

Results and discussion

Application of the in situ spectroelectrochemical cell to the study of the SEI layer

In this section, we elucidate the application of the in situ spectroelectrochemical cell with examples of the effect of salt type and electrolyte temperature on the chemical composition and structure of the SEI layer.

Application to the study of the effect of salt type on the SEI layer

Figures 2 and 3 show the in situ FT-IR spectra obtained from the porous graphite electrode of PVDF-bonded Lonza KS-44 using the new spectroelectrochemical cell at the applied potential E in 1 M $LiAsF_6$-EC/DEC solution and 1 M $LiPF_6$-EC/DEC solution, respectively. The in situ FT-IR spectrum obtained from the porous graphite electrode at open circuit potential (OCP) was used as a background spectrum to eliminate the solvent peaks from the in situ FT-IR spectra measured at E.

The $ROCO_2Li$ peaks were observed around 1645, 1300 and 1080 cm^{-1}. The pronounced peaks around 700 and 830 cm^{-1} are indicative of an As-F bond and a P-F bond, respectively. It was reported [19, 23] that the IR peak of Li_2CO_3 around 890 cm^{-1} can hardly be observed due to the "masking effect" of the solvent. However, in this work, it is possible to observe Li_2CO_3 peaks around 890 as well as 1479 cm^{-1} using the new designed in situ cell with an optimized path of the IR beam. From the FT-IR spectra obtained from the new in situ cell, it is borne out that the "masking effect" of the EC/DEC solvent is considerably reduced.

The absorbance of the $ROCO_2Li$ and Li_xAsF_y peaks increased monotonically with decreasing E in $LiAsF_6$-EC/DEC solution. However, in $LiPF_6$-EC/DEC solution the absorbance of the peaks increased with decreasing E down to 0.8 $V_{Li/Li+}$ and then decreased. It should be noted that the potential dependence of the absorbance intensity of Li_2CO_3 is fairly consistent with that of $ROCO_2Li$, irrespective of the electrolytic solution. The relative amount of $ROCO_2Li$, Li_xAsF_y and Li_xPF_y formed between the porous graphite electrode and 1 M $LiAsF_6$- and 1 M $LiPF_6$-EC/DEC solutions was estimated as a function of E by integrating the

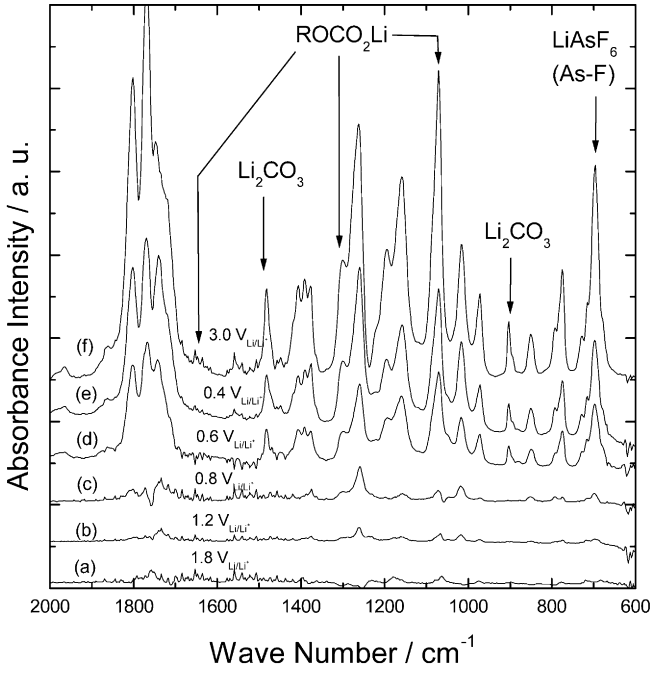

Fig. 2 The in situ FT-IR spectra obtained from the Lonza KS-44 porous graphite electrode in 1 M $LiAsF_6$-EC/DEC solution just after holding the respective potential E for 1 h, preceded by 1 h at OCP: (*a*) OCP to 1.8 $V_{Li/Li+}$; (*b*) 1.8–1.2 $V_{Li/Li+}$; (*c*) 1.2–0.8 $V_{Li/Li+}$; (*d*) 0.8–0.6 $V_{Li/Li+}$; (*e*) 0.6–0.4 $V_{Li/Li+}$; (*f*) 0.4–3.0 $V_{Li/Li+}$

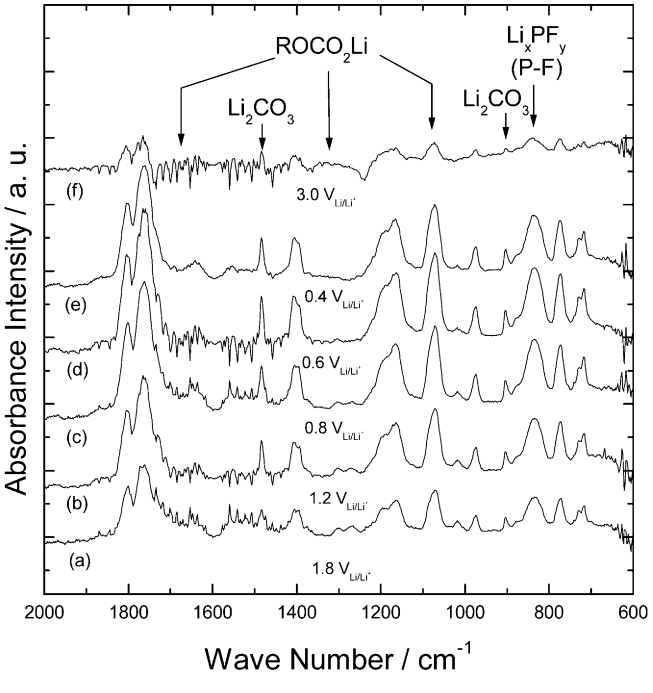

Fig. 3 The in situ FT-IR spectra obtained from the Lonza KS-44 porous graphite electrode in 1 M $LiPF_6$-EC/DEC solution just after holding the respective potential E for 1 h, preceded by 1 h at OCP: (*a*) OCP to 1.8 $V_{Li/Li+}$; (*b*) 1.8–1.2 $V_{Li/Li+}$; (*c*) 1.2–0.8 $V_{Li/Li+}$; (*d*) 0.8–0.6 $V_{Li/Li+}$; (*e*) 0.6–0.4 $V_{Li/Li+}$; (*f*) 0.4–3.0 $V_{Li/Li+}$

Table 1 In situ FT-IR qualitative analysis of the surface film formed on the porous graphite electrode in $LiAsF_6$-EC/DEC solution and $LiPF_6$-EC/DEC solution as a function of potential E and OCP

$E/V_{Li/Li+}$	Absorbance intensity (arbitrary units)			
	$ROCO_2Li$ in $LiAsF_6$-EC/DEC solution	Li_xAsF_y in $LiAsF_6$-EC/DEC solution	$ROCO_2Li$ in $LiPF_6$-EC/DEC solution	Li_xPF_y in $LiPF_6$-EC/DEC solution
1.8	4.89	4.92	0.48	0.45
1.2	5.20	5.31	1.15	1.06
0.8	5.13	4.95	1.77	1.74
0.6	9.21	8.79	1.69	1.86
0.4	11.35	11.15	1.68	1.45
OCP	18.94	18.46	0.63	0.62

measured in situ FT-IR spectra shown in Figs. 2 and 3 with respect to wave number. The results of the in situ FT-IR analysis are summarized in Table 1.

In 1 M $LiAsF_6$-EC/DEC solution, as E decreased down to 0.8 $V_{Li/Li+}$, the relative amount of $ROCO_2Li$ remained nearly constant, and then increased abruptly. It is noted that the amount of Li_xAsF_y showed the same potential dependence as that of $ROCO_2Li$. The abrupt increase in the amounts of $ROCO_2Li$ and Li_xAsF_y in 1 M $LiAsF_6$-EC/DEC solution is indicative of the onset of the electrochemical reduction of EC and $LiAsF_6$ salt at 0.8 $V_{Li/Li+}$. The relative amount of $ROCO_2Li$ increases clearly after suspending at 3.0 $V_{Li/Li+}$ for 1 h, preceded by a potential step from 0.4 to 3.0 $V_{Li/Li+}$. During the suspending at 3.0 $V_{Li/Li+}$, the decomposition of $ROCO_2Li$ formed on the porous graphite electrode at 0.4 $V_{Li/Li+}$ is preceded by its sedimentation, which means the formation of the compact $ROCO_2Li$ layer in 1 M $LiAsF_6$-EC/DEC solution.

However, the relative amounts of $ROCO_2Li$ and Li_xPF_y on the porous graphite electrode in 1 M $LiPF_6$-EC/DEC solution increased monotonically with decreasing E down to 0.8 and 0.6 $V_{Li/Li+}$, respectively, and then decreased further. It should be noted that the amounts of $ROCO_2Li$ and Li_xPF_y markedly decreased during the holding at 3.0 $V_{Li/Li+}$. The reduction in the amount of $ROCO_2Li$ with falling E below 0.8 $V_{Li/Li+}$ is due to the interference of $LiPF_6$ reduction with the compact sedimentation of $ROCO_2Li$ [19, 24]. The reduced amount of $ROCO_2Li$ during the holding at 3.0 $V_{Li/Li+}$ for 1 h showed that the sedimentation of $ROCO_2Li$ formed at 0.4 $V_{Li/Li+}$ just follows its decomposition in 1 M $LiPF_6$-EC/DEC solution.

From the comparison of the potential dependence of the relative amount of $ROCO_2Li$ and salt reduction products formed in 1 M $LiAsF_6$-EC/DEC solution with that in 1 M $LiPF_6$-EC/DEC solution, it is strongly suggested that the electrochemical reduction reactivity of $LiPF_6$ salt is lower than that of $LiAsF_6$ salt.

Application to the study of the effect of electrolyte temperature on the SEI layer

Figure 4 presents the in situ FT-IR spectra measured on the porous graphite electrode of PVDF-bonded SLX6 using the new in situ spectroelectrochemical cell under the application of a potential of 0.7 $V_{Li/Li+}$ in 1 M $LiPF_6$-EC/DEC solution at 0 °C for various times. Under the application of the SEI formation potential of 0.7 $V_{Li/Li+}$ to the porous graphite electrode, all the FT-IR spectra peaks concerning $ROCO_2Li$ and Li_2CO_3 and the P-F bond in the FT-IR spectra increased with time without any marked changes in peak positions. These FT-IR spectra show that the SEI formation reaction still proceeds after 1 h at 0.7 $V_{Li/Li+}$ and 0 °C due to the reduction of the 1 M $LiPF_6$-EC/DEC electrolyte, indicating that the reactions run kinetically rather sluggishly at the electrolyte temperature of 0 °C.

Figure 5 shows the in situ FT-IR spectra measured on the porous graphite electrodes of PVDF-bonded SLX6 under the application of the SEI formation potential of 0.5 $V_{Li/Li+}$ for 2 h in 1 M $LiPF_6$-EC/DEC solution at different SEI formation temperatures of 0, 20 and 35 °C, respectively. The peak positions of $ROCO_2Li$, Li_2CO_3

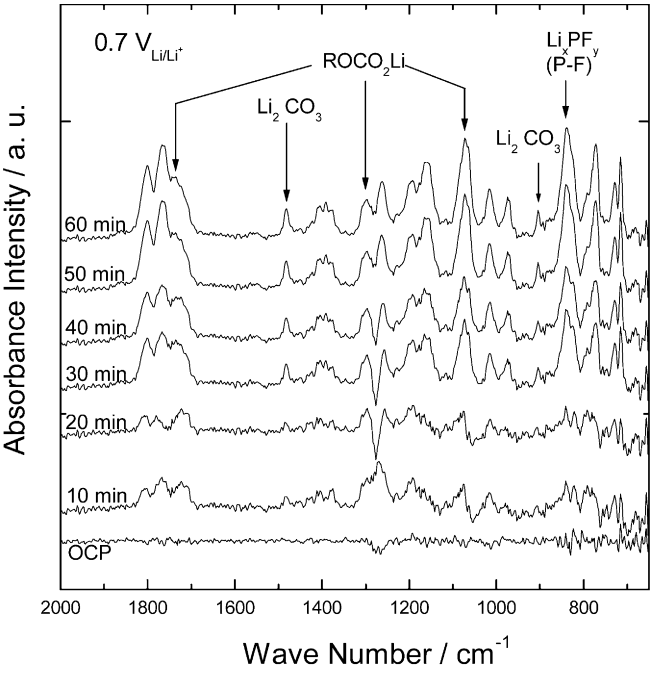

Fig. 4 The in situ FT-IR spectra measured on the SFG 6 porous graphite electrode subjected to an applied potential of 0.7 $V_{Li/Li+}$ in 1 M $LiPF_6$-EC/DEC solution at 0 °C for various times

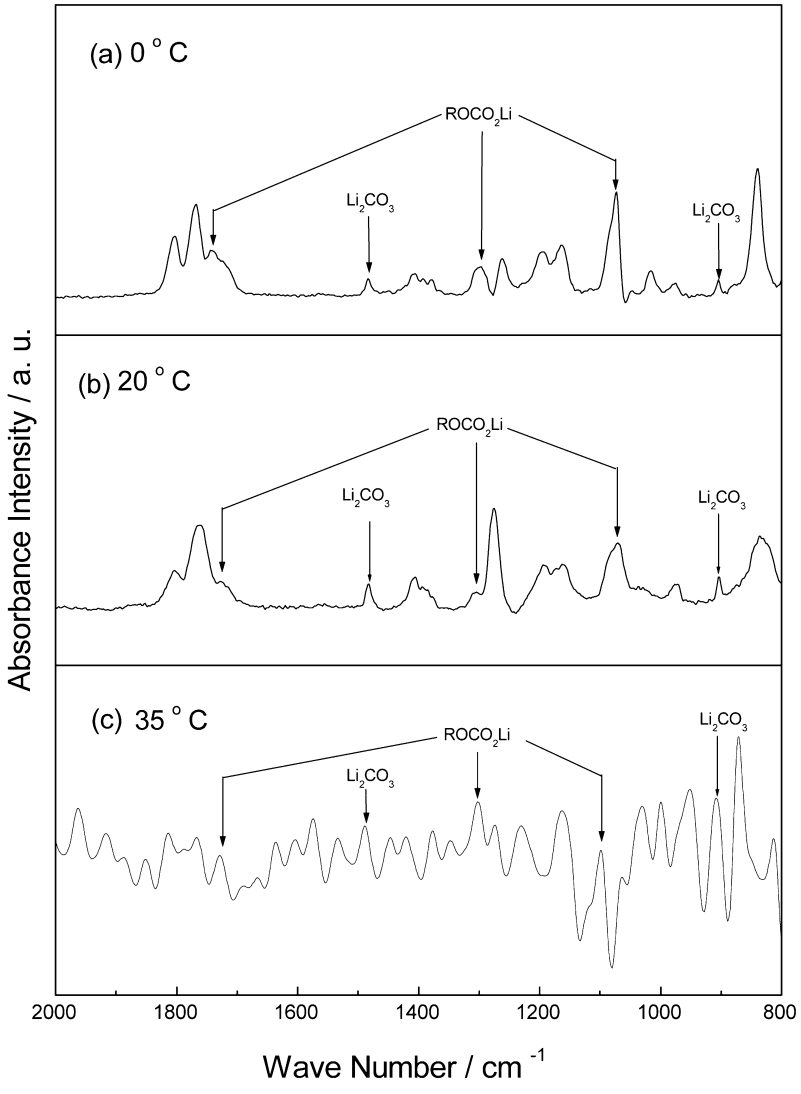

Fig. 5 The in situ FT-IR spectra measured on the SFG 6 porous graphite electrodes subjected to an applied potential of 0.5 $V_{Li/Li+}$ for 2 h in 1 M $LiPF_6$-EC/DEC solution at different SEI formation temperatures: (*a*) 0 °C; (*b*) 20 °C; (*c*) 35 °C

and the P-F bond remained nearly unchanged, regardless of the SEI formation temperature. The relative amount of Li_2CO_3 to $ROCO_2Li$ was obtained by integrating the corresponding peak of the FT-IR spectra in Fig. 5. The result is summarized in Table 2.

In general, EC is a highly reactive solvent and, therefore, when it is a major component in an electrolyte solution, its reduction dominates the lithiated graphite surface chemistry and suppresses other reactions, such as those of CO_2 or CO on the active electrode surface [25, 26, 27]. This means that, during the SEI formation, Li_2CO_3 is not formed by the direct reduction of CO_2 or CO gas on the graphite surface, but it is formed by further reduction of $ROCO_2Li$ which is a direct reduction product of EC.

Thus, the increased relative amount of Li_2CO_3 to $ROCO_2Li$ accounts for the enhanced transformation of $ROCO_2Li$ to Li_2CO_3 with rising SEI formation temperature. Moreover, it is noted that the transformation of $ROCO_2Li$ into Li_2CO_3 is accompanied by the following additional gas evolution reactions [26, 27]:

$$2ROCO_2Li + H_2O \longrightarrow Li_2CO_3 + 2ROH + CO_2 \uparrow \quad (3)$$

$$2ROCO_2Li + 2e^- + 2Li^+ \longrightarrow 2Li_2CO_3 + CH_2{=}CH_2 \uparrow \quad (4)$$

In an EC-based electrolyte, R corresponds to CH_2.

As a result, additional gas evolution reactions are enhanced with rising SEI formation temperature, and hence the number of defect sites in the SEI layer is

Table 2 The relative amount of Li_2CO_3 to $ROCO_2Li$ formed on the porous graphite electrode exposed to 1 M $LiPF_6$-EC/DEC solution at 0.5 $V_{Li/Li+}$ for 2 h with respect to SEI formation temperature

SEI formation temperature (°C)	Relative amount of Li_2CO_3 to $ROCO_2Li$
0	0.063
20	0.219
35	0.602

increased with rising SEI formation temperature. It is reasonable to say that as a result of enhanced gas evolution during the SEI formation reaction, the number of defect sites in the SEI layer increased with rising SEI formation temperature.

Judging from the experimental results obtained from this work, the new in situ FT-IR spectroelectrochemical cell allows us to detect qualitatively the chemical composition and structure of the SEI layer formed between the porous graphite electrode and the alkyl carbonate solution, without any contribution of atmospheric contaminants.

Conclusions

This article critically evaluates the characteristics of a new in situ spectroelectrochemical cell with an optimized path of the IR beam, designed in our laboratory for the study of the chemical composition and structure of the SEI layer between the porous graphite anode and alkyl carbonate solution, which is conceptually similar to the ''thin layer electrolyte configuration'' cell. The in situ cell is designed in view of the incident IR beam angle that it gives such a short depth of 0.277–2.77 μm of penetration of the evanescent IR beam through the ATR crystal into the electrolytic solution. This enables us to minimize the ''masking effect'' of the EC/DEC solvent.

Moreover, the ''local compositional change'' which may arise significantly from the ''thin layer electrolyte configuration'' cell also can be quite circumvented, since only the electrolyte in the vicinity of the electrode composed of the graphite particles is reduced to form the SEI layer to a thickness of at most 0.1 μm during the application of potentials.

In these respects, the designed in situ cell proved to be a reliable and powerful tool for investigation of the chemical composition and structure of the SEI layer. As examples for the application of the designed in situ cell, we elucidated the effect of salt type and electrolyte temperature on the chemical composition and structure of the SEI layer between the graphite particles and EC/DEC solution with the help of various measured in situ FT-IR spectra.

Acknowledgements The receipt of a research grant under the internal research programme ''Technological Development of High Performance Lithium Battery'' from the Korea Advanced Institute of Science and Technology (KAIST) 2000/2002 is gratefully acknowledged. This work was partly supported by the Brain Korea 21 project.

References

1. Neugebauer H, Nauer G, Konopik NB, Gidaly G (1981) J Electroanal Chem 122:381
2. Ozanam F, Chazalviel JN (1988) Rev Sci Instr 59:242
3. Ozanam F, Djebri A, Chazalviel JN (1996) Electrochim Acta 41:687
4. Russell AE, Rubasingham L, Hagans PL, Ballinger TH (1996) Electrochim Acta 41:637
5. Zhu XY, Yan DY, Fang YP (2001) J Phys Chem B 105:12461
6. Surca A, Orel B, Drazic G, Pihlar B (1999) J Electrochem Soc 146:232
7. Hartl F, Luyten H, Nieuwenhuis HA, Schoemaker GC (1994) Appl Spectrosc 48:1522
8. Ping Z, Neugebauer H, Neckel A (1996) Electrochim Acta 41:767
9. Best SP, Clark RJH, McQueen RCS, Cooney RP (1987) Rev Sci Instrum 58:2071
10. Klima J, Kratochvilova K, Ludvik J (1997) J Electroanal Chem 427:57
11. Kulesza PJ, Malik MA, Denca A, Strojek J (1996) Anal Chem 68:2442
12. Iwasita T, Nart FC (1997) Prog Surf Sci 55:271
13. Bewick A, Kunimatsu K, Pons BS (1980) Electrochim Acta 25:465
14. Bewick A, Kunimatsu K (1980) Surf Sci 101:131
15. Nichols RJ, Bewick A (1988) Electrochim Acta 33:1691
16. Zhang J, Lu J, Cha C, Feng Z (1989) J Electroanal Chem 265:329
17. Roth JD, Weaver M (1991) Anal Chem 63:1603
18. Aurbach D, Chusid P, Weissman I, Dan P (1996) Electrochim Acta 41:747
19. Pyun S-I, Ryu Y-G (1998) J Electroanal Chem 455:11
20. Pyun S-I (1999) Fresenius J Anal Chem 363:38
21. Fishbane PM, Gasiorowicz S, Thonton ST (1996) Physics for scientists and engineers. Prentice Hall, Englewood Cliffs, NJ, p 973
22. Griffiths PR, Haseth JA (1986) Fourier transform infrared spectroscopy. Wiley, New York, p 194
23. Ein-Eli Y, Markovsky M, Aurbach D, Cameli Y, Yamin H, Luski S (1994) Electrochim Acta 39:2559
24. Aurbach D, Gofer Y, Benzion M, Aped P (1992) J Electroanal Chem 339:451
25. Ryu Y-G, Pyun S-I (1997) J Electroanal Chem 433:97
26. Aurbach D, Markovsky B, Weissman I, Levi E, Ein-Eli Y (1999) Electrochim Acta 45:67
27. Lee S-B, Pyun S-I (2002) Carbon (in press)